



Investigation of K, Th, U in Multiple Hoarded Granites and their Effects in the Environment using LIBS Coupled with Chemometric Technique



Shukla VK¹, Abhishek Kr Rai², Rajneesh Kumar Verma¹ and Rai AK^{1*}

¹Laser Spectroscopy Research Laboratory, Department of Physics, University of Allahabad, India

²Department of Earth and Planetary Science, University of Allahabad, India

Submission: May 01, 2023; **Published:** June 16, 2023

***Corresponding author:** Rai AK, Laser Spectroscopy Research Laboratory, Department of Physics, University of Allahabad, Prayagraj-211002, India, Email: awadheshkrai@rediffmail.com

Abstract

The present manuscript deals with the consequences of radioactive elements present in multiple hoarded granites on the environment using the Laser-induced breakdown spectroscopy technique. To the best of our knowledge, the occurrence of radioactive elements has been correlated with the geochemical model for the first time. The spot-wise detection of Granite using the point detection capability of the LIBS technique confirms the radioactive elements such as K40, Th, and U along with some other common elements such as Si, Mg, Fe, Ti, Al, Ca, and Li. The various colors present in each spot are explained based on the elements present in each spot. To characterize the quality of the Granite, the hardness of each spot has been calculated by LIBS spectral lines and compared with the conventional mechanical hardness technique such as the Mohs hardness test. An attempt has been made to explain the hardness of the granite with the geochemical model of radioactive elements. The hardness of each spot has been again allied with the plasma temperature and plasma electron density with appropriate explanation. The chemometric technique such as principal component analysis (PCA) and Hierarchy clustering analysis (HCA) has been employed to distinguish each spot qualitatively and quantitatively, both techniques are found in good agreement, and the results are equally supporting the result obtained by the LIBS technique.

Keywords: Multiple Hoarded Granites; LIBS; Geochemical Model; Hardness; Plasma Parameter HCA; PCA

Abbreviations: PCA: Principal Component Analysis; HCA: Hierarchy Clustering Analysis; LIBS: Laser-Induced Breakdown Spectroscopy

Introduction

Granites, light-colored plutonic rocks, are found as igneous rocks in nature. Igneous rocks may be Archean or post-Archean depending upon whether it is high metamorphism, volcanic process, or light metamorphism, volcanic process respectively [1]. Granite is generally found in gleaming color and has different morphology in nature which depends on the climate, soil, etc. El-Taher et al. detected Na, Mg, K, Fe, Sc, Cr, Ti, Al, As, Fe, Mn Co, Zn, Ga, Rb, Zr, Nb, Sn, Ba, La, Ce, Nd, Sm, Eu, Yb, Lu, Hf, Ta, Pb, V, Th, and U in the granite rocks collected from the Aswan area in Southern Egypt [2]. Similarly, Umar et al. found emission lines of Si, Ca, K, Fe, Mg, Al, Na, and Li in the raw granite rocks acquired from deposits in the Hunza district, Gilgit area of Pakistan [3]. Rock/Mines experts are very curious to identify before the exploitation of specific rocks (Granite) because it is necessary to inspect the constituents, nature, and features of the rock mass present in

quarries and mines by mechanical fragmentation [4]. However, the design of mechanical equipment for fragmentation, hauling, drilling operations, and crushing depend to a large extent on the quality and quantity of textural characteristics data. It helps the mine managers in the selection of appropriate machinery for their different levels of procedure and initiate the optimum act of the equipment. The disparity in the resistance experience on different rock types is subject to the textural characteristics of the rocks [5]. Granites are molded according to the variability of the supplies from exterior decoration to the interior like flooring tiles, Kitchen counters, etc. [6]. For use in artificial jewelry as well as for building materials, spectacular and striking Granites from Gilgit-Baltistan deposits are being used in India as well as exported to Saudi Arabia, China, Russia, the Middle East, the United States, Malaysia, and other countries [7].

Many researchers appealed that the application of Granite can conceivably be a source of harmful radiation as it encompasses some hazardous trace radioactive elements [8], it may contain ~0.5–4.7 ppm of Uranium(U), ~1.6-10.7 ppm of Thorium(Th) and ~37–1100 ppm of radioactive potassium [9]. These radioactive elements are producing heat in the environment and are the cause to global warming, so it is burning necessity to address the radioactive property of Granite rock sample as well. Granitic rocks are unique among common rock types in having high concentrations of heat-producing radioactive elements, namely U, Th, and K [10]. The origin of heat-producing and other large-ion lithophile(LIL) elements is from the middle and upper crustal levels of the earth, they may transport through various processes associated with high-grade metamorphism, metasomatism, and partial melting [8]. Potassium (LIL elements) has been found in Granites as an essential element of common rock-forming minerals as phlogopite, biotite and muscovite. Uranium (U) and Thorium (U) are also LIL elements, but because of their lower abundance, they are present mostly in trace amount in common rocks [11]. On the whole, the chemical behavior of U, Th and K is unequal, but all three being LIL elements, they show similar inclinations in large-scale processes. Geochemical and Cosmochemical models predict the global mean ratios of occurrence as given by following relation [8]:

$$K/U = (1.0-1.3) \times 10^4 \text{ and } Th/U = (3.7-4.0)$$

In the present manuscript, the above-mentioned ratio of the radioactive elements is verified by the LIBS technique. LIBS is based on emission spectroscopy and the details of this promising technique is discussed below.

Laser-induced breakdown spectroscopy (LIBS) has emerged as a subtle and consistent optical emission technique that is being used to investigate the elemental compositions of materials in the solid, liquid, or gaseous form [12-14]. In this technique, when given sample is irradiated with a high-power pulsed laser, the material is heated and get melted which forms a plasma plume that consists of atom, ions and electrons, such that the laser fluence is greater than the breakdown threshold of the material. The material ablation should be stoichiometric under the LIBS conditions, and finally, the identification and quantification of the species are achieved by examining the atomic and ionic lines emitted by the laser-produced plasma. It has been observed that the intensity of the atomic emission spectrum of a given materials in LIBS also depends on the matrices (hardness) of solid substances [13,15].

The hardness of a material is characterized by its resistance to permanent indentation and there are several hardness tests that can be used [16,17]. One of the most commonly employed techniques is the Vickers hardness test, Mohs hardness test etc. which requires the optical measurement of the indented area related to an applied load, these tests can be time-consuming,

places geometric and size constraints on the samples and requires that samples have a good surface finish [18].

The laser-Induced Breakdown Spectroscopy (LIBS) technique has been successfully employed to determine the surface hardness of various solid samples which have different degrees of humidity such as concrete samples [19]. Z. Abdel Salam et al. [20] used the LIBS technique to measure the surface hardness of calcified tissues. They reported that in calcified tissues, the intensity ratios of Ca II / Ca I and Mg II / Mg I gave a direct correlation with the sample's surface hardness of different types and demonstrated that there is a remarkable correlation between the surface hardness of solid samples and the intensity ratio of ionic to atomic emission spectral lines from the plasma. Additionally, the laser-induced plasma parameters, namely the electron density and the plasma excitation temperature have been estimated as a function of the surface hardness of the selected samples [21]. The obtained direct proportionality between the plasma temperature and the sample's surface hardness is due to the increased collisions in the plasma plume because of strong repulsive forces for harder targets [22]. Since the selected Granite sample is consisting of multiple spots having various colors and various surface morphology so it is necessary to apply chemometric technique to differentiate qualitatively.

Principal component analysis (PCA) and Hierarchy clustering analysis (HCA) techniques are used to differentiate each spot present in Granite rock sample. In one side where, PCA works by taking large number of data sets for each spot and form it co variant matrix finally grouped in 2D or 3D spaces according to the excess or trace amount of elements present in each spot whereas HCA may be applied to that sample where large data sets matrix (observations) are not necessary [23]. PCA and HCA are both unsupervised technique and both are used frequently to distinguish the sample in modern spectroscopy technique data set.

Therefore, the foremost objective of the present paper is to evaluate the practicability of the measurement, via the LIBS technique, of the radioactive elements and their environmental effect in multiple hoarded granite. Many other elements such as Si, Mg, Fe, Ti, K, Sr, Ba etc. have been detected and the colour with surface appearance of each spot has been explained based on the relative intensity of the spectral lines of these elements. The relative surface hardness of the sample has been calculated to characterize the Granite sample of each spot and correlated with the Mohs hardness test which has been found in good correlation. Plasma parameter such as plasma temperature and plasma electron density also vary with sample matrix(hardness) which is also explained well. Chemometric technique such as PCA and HCA is applied well to distinguish each spot both results are in close agreement and explain/support well to the results obtained by the LIBS technique.

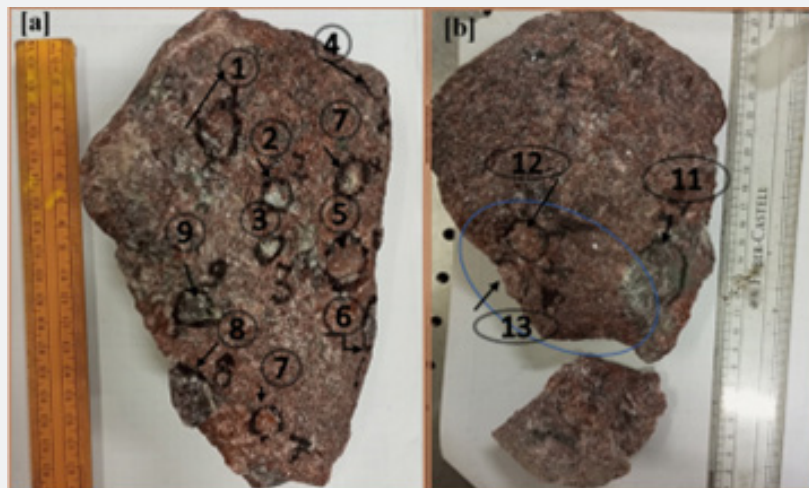


Figure 1: [a] Photograph of the total Granites and [b] Annular part is encircled by blue color.

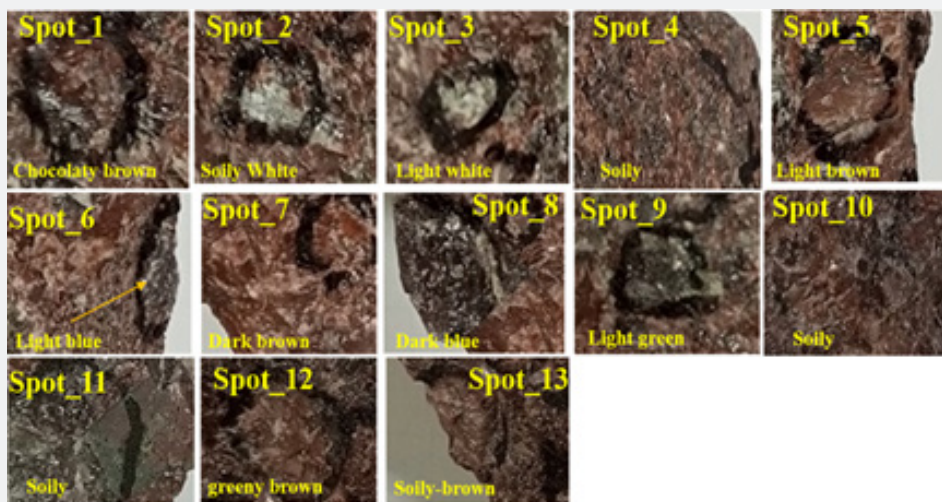


Figure 2: Resolved image of each spot of the big granite sample.

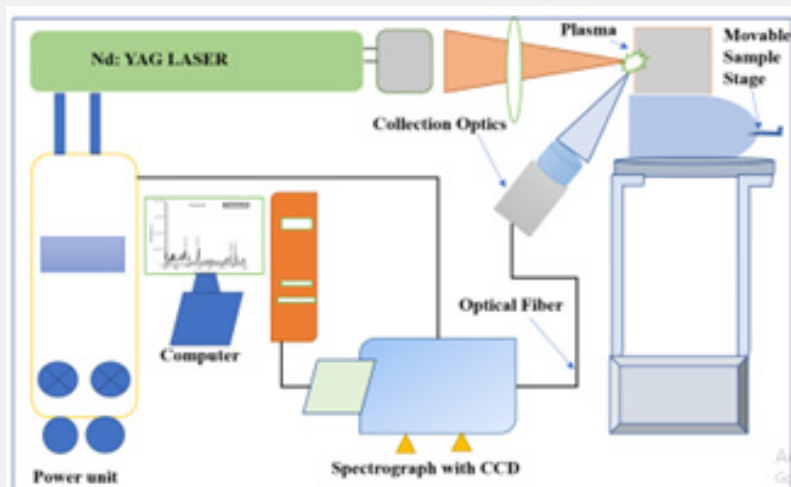


Figure 3: Experimental set-up for recording LIBS spectra of granite sample.

Materials and Methods

Sample preparation

The photograph of the bigger size of the Granite sample is shown in Figure 1. The Granite sample is collected from the mining area of the district Mirzapur (U.P) India. In the shown sample of Granite, we have marked total thirteen spots including the annular region these spots have different colors and different surface morphology. To better understand the color of each spot and surface morphology, we have shown the resolved image of each spot in Figure 2.

Experimental technique

The elemental configuration/identification of the granite samples is examined by optical emission spectroscopy i.e., LIBS. The elemental composition has been obtained by inspecting the optical emission spectra of the laser-produced plasma which was produced on the surface of the Granite sample. The experimental set-up is shown in Figure 3 which consists of a high-power Q-switched Nd: YAG laser (Continuum, Surelite III-10 USA) having 4 ns pulse duration and 10 Hz repetition rate, which can deliver maximum energy of about 425 mJ at 532 nm. An energy meter (Genetec-e model UP19K-30H-VM-DO) was used to measure the laser pulse energy. A quartz lens (convex) of 10 cm focal length and a collection optics (UV-NIR light collection ME OPT007, Andor Technology, USA) was used to focus the laser beam on the target sample placed in air at atmospheric pressure and collect the light from the plasma. The plasma was generated by focusing the Nd: YAG laser beam with pulse energy of about 15 mJ at 532 nm and a laser spot size of about 0.5 mm after focusing, which corresponds to the laser fluence of $\sim 65 \text{ J/cm}^2$. The target sample was placed on a rotatable stage to prevent crater formation and to provide a fresh location for the target sample. The spectrometer provides high resolution (FWHM of 0.1 nm) in the 200–510 nm region and low resolution (FWHM of 0.75 nm) in the wavelength region 200–900 nm.

Result and Discussion

Qualitative analysis of LIBS spectra

(Figure 1a-b) is big granite marking of the thirteen spots. and Figure 2 is resolved image of each spots showing different color and texture.

A typical optical emission spectrum (Figure 4) consists of spectral lines of the constituent elements, which provides information about the major and trace elements present in the Granite sample. In Figure 4, we show the optical emission spectrum of granite rock in different spots covering the wavelength range from 240 to 500 nm.

The average spectrum of ten laser shots was recorded to avoid the surface inhomogeneity and to minimize the statistical errors. The spectral lines belonging to various elements in the spectra were identified with the help of the NIST database [24].

The emission spectra mainly consist of dominant spectral lines of Si, Ca, K, Fe, Mg, Li and Al along with the trace elements such as Sr, Ba U, Th. The spectrum in the wavelength region (265–310 nm) mainly contains lines of Fe, Ti, and Al along with a Si line. Some of the fine persistent line of radioactive elements such as Th and U, K along with Li are shown in following LIBS spectra (Figure 5).

The radioactive element Th line appeared at wavelength 330.4(I), 360.9(II), 370.6(I), 371.9(I), 382.8(I) etc. as shown in (Figure 5a), U at wavelength 348.9(I), 351.4(I), 356.1(I), 356.6(I), 358.4(I), 383.9(I), 385.4(I) etc. as shown in (Figure 5b), K at wavelength 766.4(I), 769.8(I) etc, as shown in (Figure 5c) and Li at wavelength 610.3(I), 670.7(I) as shown in (Figure 5d) respectively.

Analysis of the responsible elements present in the color of each spot

On observing closely, the colors of each spot are found to be different from each other. Therefore, it is necessary to find out the responsible elements for the appearance of the color. Spot_1 Mg and Fe are responsible for the silvery colour and chocolaty colour. Spot_2 contains Mg and Si therefore, it looks like silver white in spot_3 Ca, Fe is present along with the Si element so this spot is light white however the spot_3 consist of an ample amount of Fe but still it is light white because of the excess amount of the Ca element is present as shown in Figure 6.

Similarly, we may explain the color appearance of the remaining spots. The summary of the responsible elements of each spot has been given in Table 1.

Estimation of the relative hardness

As we discussed in the introduction section that hardness(resistance) is crucial property to distinguish the type of Granite. Hardness is the ability of a material to resist deformation, and it, generally, is determined by the conventional test (Mohs hardness, Vickers hardness, etc.) where the surface resistance to indentation is measured. This commonly used method of hardness tests is defined by the shape or type of indent, the size and the amount of load applied which is not an easy task. Now-a-days, LIBS technique is frequently used to determine the hardness just by taking the ratio of ionic to atomic line (for example CaII (393.3)/CaI (422.7)) provided that the selected spectral lines should not be self-absorbed. To confirm that the selected lines is not self- absorbed, we have calculated partial self-absorption coefficient ($KR(\lambda)$ (in $\text{m}^2 \text{ s}^{-1}$)) of the lines.

It can be obtained by multiplying the self-absorption cross-section (S_L) of such line with the lower energy level population (C):

$$KR(\lambda) = S_L \cdot C$$

$$S_L = 0.33\lambda_0 \sqrt{\frac{m}{T}} \frac{g_j}{g_i} A_{ji}$$

where C is given by:

$$KR(\lambda) = 1.85001E - 5 m^2 s^{-1}$$

where λ_0 is the wavelength of the spectral line (in m), M is the atomic mass of the element, g_i and g_j are the statistical weights of the lower and upper levels, respectively, T is the temperature (in K), and A_{ji} is the transition probability (in s^{-1}), U is the partition function, E_i is the energy of the lower energy level, and K_b is the Boltzmann's constant. For this purpose, we have placed respective value of each parameters of the selected lines (CaI & CaII) and

calculated the partial self-absorption coefficient for CaII at 393.6 nm, and CaI at 422.9 nm and found $KR(\lambda) = 1.85001E - 5 m^2 s^{-1}$ for CaII and $9.50078E - 5 m^2 s^{-1}$ for CaI respectively. The selected calcium lines in our measurements have relatively low partial self-absorption coefficient than calculated by Authors K. Tsuyuki et al. which are found for CaII at 396.8 nm and CaI at 422.6 nm are $1.9618 E - 5$ and $9.6607E - 5 m^2 s^{-1}$ respectively [22].

Now, taking the ratio of ionic and atomic lines calcium elements we have plotted the bar plot showing the hardness of each spot.

Table 1: Spot location, its colour and corresponding responsible elements.

Sr.no.	Spot location	Spots color	Responsible elements
1	Spot_4	Soily	Si, Ca
2	Spot_5	Light brown	Fe, Fe
3	Spot_6	Light blue	Ti, Fe
4	Spot_7	Dark blue	K, Li
5	Spot_8	Green	Fe, Si
6	Spot_9	Light green	Fe, K
7	Spot_10	Light soily	Si
8	Spot_11	Soily	Si, Ca
9	Spot_12	Green- brown	Fe, K, Ti
10	Spot_13	Soily	Si, Ca

Table 2: Average of the relative intensity of different radioactive elements (Th, U, K) and their ratios.

Spot Group	Averaged value of Th (371.9)	Averaged value of U (385.8)	Averaged value of K -766.5	K/U x 10 ⁴	Th/U
Group_I	13.34	24.97	583.7	0.002356	0.56
Group_II	8.17	13.54	1919.48	0.01417	0.6
Group_III	9.69	13.67	2052.31	0.015013	0.7

As we observe the bar plot (Figure 7) for the hardness of each spot of granite, we may categorize each spot in three groups. Group_I has spot_3, 6, and 11 with maximum hardness(highest). Group_II has spot_1,2,4,9,10,13 with moderate hardness(medium) and Group_III have spot_5,7,8,12 with minimum hardness (Low). The variation of hardness depends upon various factors such as grain size, crystallization condition, rolling temperature, crystal structure and their interatomic/bonding force etc. [25,26]. The reliability of the relative hardness calculated by the LIBS technique is validated further by applying the Mohs hardness test as discussed below.

Relation between Mohs hardness and LIBS hardness

The Mohs hardness is assigned with in the value between 1 and 10. The larger the value, the harder will be the given mineral. Mohs hardness scale is the arrangements of ten reference minerals. In this test the hardness of minerals is defined as their resistance to being scratched [27]. So, by doing the successive test

with reference successive reference specimens, we can closely estimate the Mohs hardness of the given minerals.

Figure 8 represents the correlation plot between the hardness measured by the LIBS technique (Intensity ratio) and measured Mohs hardness. The coefficient of determination ($R^2 = 0.9686$) suggests that both techniques are indicating consistency in the result. In Figure 8, we see that three groups of hardness (highest, medium and minimum) are similar as calculated by LIBS technique hardness (Figure 7). Furthermore, Mohs hardness test requires scratching in the surface so it is destructive therefore hardness measured by the LIBS technique is the best technique to monitor the surface hardness of the samples because it is non-destructive to the surface, real-time, portable, in-situ system and can be used under extreme conditions such as encountered in a nuclear reactor, ion accelerator or Tokamak. we may correlate the hardness of each spot based on the radioactive elements present in the granite sample as discussed in the following section.

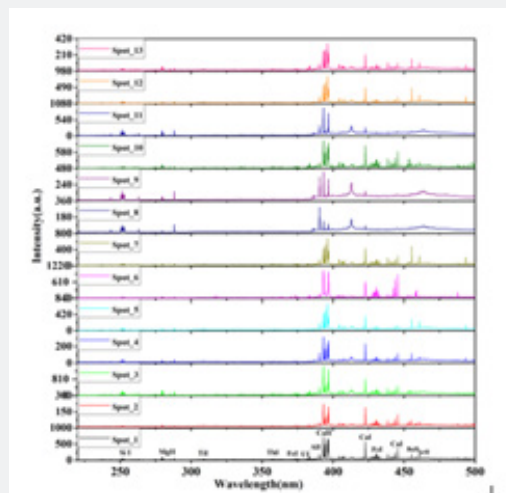


Figure 4: LIBS spectra of each thirteen spots having wavelength between 240-500nm.

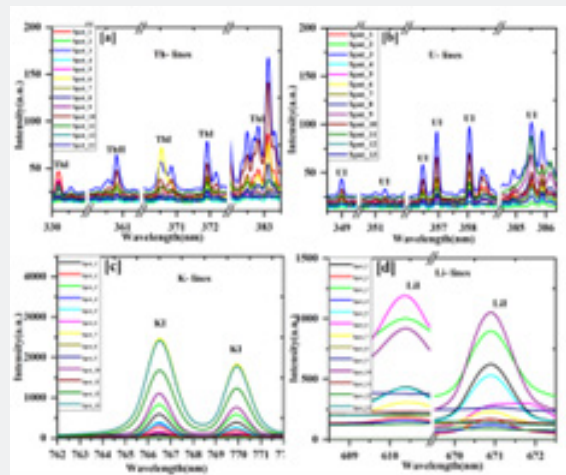


Figure 5: Persistent spectral lines of Th, U, K, and Li at different wavelengths.

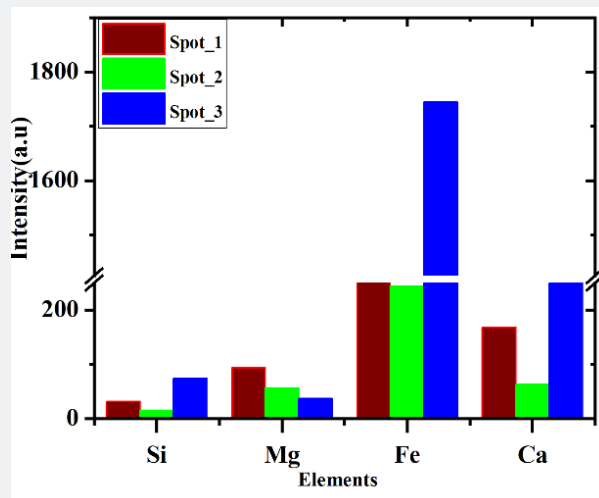


Figure 6: Relative intensity of the LIBS spectral lines of different elements.

Analysis of radioactive elements of Granite for the environmental effect

Heat production by radioactive decay is among the main heat sources on the Earth [28]. The information of heat production in granitic rocks is pivotal for the thermal modeling of the Earth's crust. Jaupart et.al. [10] found that Granitic rocks are unique among common rock types in having high concentrations of heat-producing radioactive elements, namely U, Th, and K. Rudnick et al. [2] found that, although the chemical behavior of U, Th, and K is dissimilar yet they exhibit similar tendencies in large-scale processes. Geochemical models predict the following global mean ratios of radioactive elements occurrence:

$$K/U = (1.0-1.3) \times 10^4$$

$$Th/U = (3.7-4.0)$$

Based on this model, we have also calculated the ratio of the concentration of the above-found elements using LIBS technique and tabulated them as follows (Table 2).

We have averaged the relative intensity of Th elements for Group_I spots and placed the value in the row of Group_I (Spot_3,6,11) also for U elements, we have averaged the relative intensity of Group_I spots and similarly for K element. The same procedure has been followed for Group_II and Group_III respectively. From this Table 2, we may deduce that the group of spots having the lowest hardness shows a maximum ratio of K/U and Th/U and vice-versa. Irina M Artemieva et al. [8] reported that post-Archean rocks (lightly metamorphized low-volcanic sediments) have higher concentrations of heat-producing elements (HPE) than Archean rocks (heavily metamorphized and deep-volcanic sediments). Since, Group_III spots have greater heat-producing elements i.e., HPE (K/U, Th/U) so they must have been made of post-Archean-type rocks (Granite). As we know that post-archaeon rocks are low metamorphized and volcanic sediments so it must be minimum hardness therefore from the Table 2, we may infer that Group_III has the lowest hardness. Similarly, Group_I spot are made of Archean rocks (Granite) due to minimal concentration of HPE hence these spots reflect the highest hardness. Group_II spots are showing moderate hardness which means these spots have a blend of Archean and post-Archean Rocks (Granite) due to these spots to have a moderate ratio of HPE hence indicating moderate hardness value.

To clear the relation between the hardness and the ratio of the radioactive elements we have plotted the correlation plot (Figure 9a, b).

(Figure 9a) is the correlation plot between the hardness and the Th/U. Each point represents the average of spots of one group (as Group_I, II & III) which has approximately similar ratio of the Th/U and hardness respectively. The coefficient of determination (R^2) = 0.9256 suggest that the occurrence of the radioactive

elements varies with respect to the hardness coherently. Similarly, the ratio K/U shows proportional behavior with respect to the hardness (Figure 9[b]).

Plasma Parameters

Plasma temperature and electron density of plasma are vital parameters to know the actual characteristics of the selected sample. The study shows some significant variation in this plasma parameter with respect to variation in hardness [29]. Therefore, the viability of hardness measurement via the LIBS technique for Granite samples was evaluated. This was done by measuring the value of the plasma excitation temperature (T_e) and plasma electron density (N_e) in the different spots of the granite samples.

Plasma temperature

Plasma temperature is the measure of the thermal kinetic energy per particle. Customarily, it is measured in kelvins or electron volt. The high temperatures are usually needed to sustain ionization, which is a defining feature of plasma. At low temperatures, ions and electrons tend to recombine into bound states atoms and the plasma will finally become a gas [30]. To determine the plasma temperature (T_e), the Boltzmann plot (Figure 10) method from the LIBS spectral line intensities is used. Since, the relative intensity (I_{ki}) of the spectral lines may be defined by the equation:

The Boltzmann equation:

$$\ln \left[I_{ki} / (A_{ki} g_k) \right] = \frac{-E_k}{K_B T} + \ln [F.C_S / U_s (T)]$$

comparing with the standard linear equation, it gives slope (m) and intercepts (q_s) as follows:

$$Y_k = \ln \left(I_{ki} / (A_{ki} g_k) \right), X_k = E_k, m = -\frac{1}{K_B T}, q_s = \ln [F.C_S / U_s (T)]$$

Table 3 shows the plasma temperature (T_e) from six promising selected spots by using Boltzmann plot (Figure 10). The Spot_3&11 are having maximum hardness, Spot_1&2 are having medium value of hardness and Spot_5&8 are having minimum value of hardness.

Hardness v/s Plasma temperature plot

The viability of hardness measurement via the LIBS technique for granite samples was evaluated. This was done by measuring the value of the plasma temperature (T_e) in the different sample's spots using the Boltzmann plot (Figure 10) and tabulated in Table 4.

From the above Table 4, it is obvious that the spot having a higher hardness value indicates a higher plasma temperature. To clearly understand the relation between hardness and Plasma temperature we have plotted a correlation plot (Figure 11). The coefficient of determination ($R^2 = 0.9986$) suggests that hardness of the Granite spots show proportional behavior.

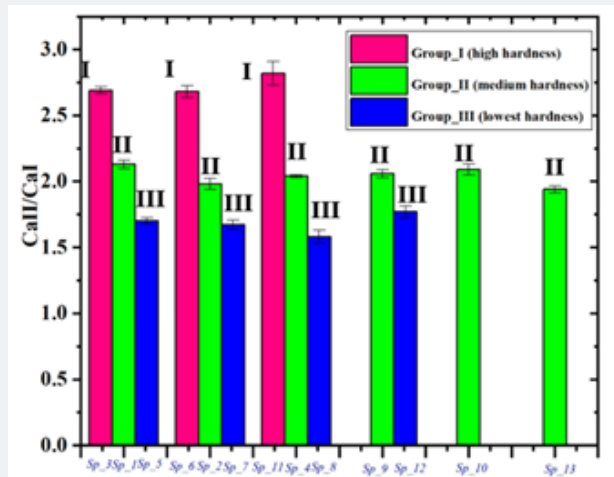


Figure 7: Hardness of the different spots from the big granite.

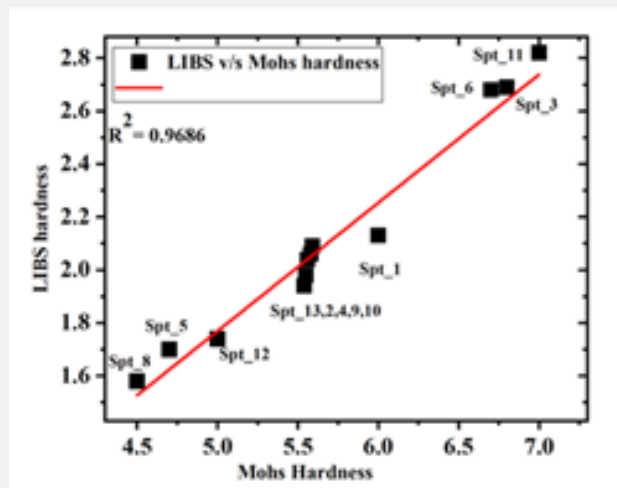


Figure 8: Correlation plot of Mohs hardness and LIBS hardness of the different spots from granite sample.

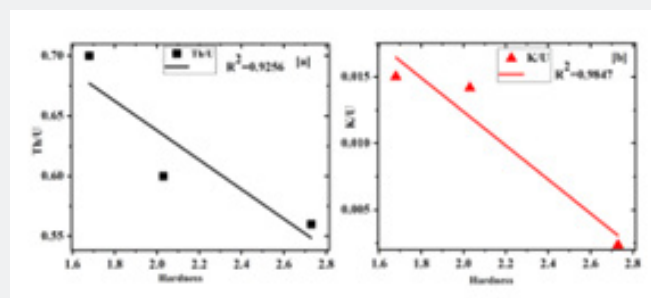


Figure 9: [a] Correlation plot Th/U, [b] K/U with hardness.

Plasma electron density

Plasma density often refers to the plasma electron density, that is, the number of free electrons per unit volume. For plasma

to exist, ionization is necessary. The plasma temperature is mainly responsible to the ionization of a plasma which depends to the atoms that have lost or gained plasma electrons density. Moreover, the electron density is related by the average charge state of the

ions and density of electrons [31].

Hardness v/s Plasma electron density plot

From studying the well-isolated line of Si(288.1nm) in the plasma emission, the electron density (N_e in cm^{-3}) can be estimated using the equation.

$$\Delta\lambda_{1/2} = 2\omega N_e / 10^{16}$$

where $\Delta\lambda_{1/2}$ and ω are the FWHM of the Si line and the electron

impact parameter respectively.

Table:5 shows the plasma electron density with respect to the hardness. From the table we may easily infer that plasma electron density increases with respect to increase in the hardness value.

The correlation plot (Figure12) shows that the harder the sample, it has more electron density of the plasma plume. $R^2=0.9928$ suggest that it is in good correlation with hardness and electron density.

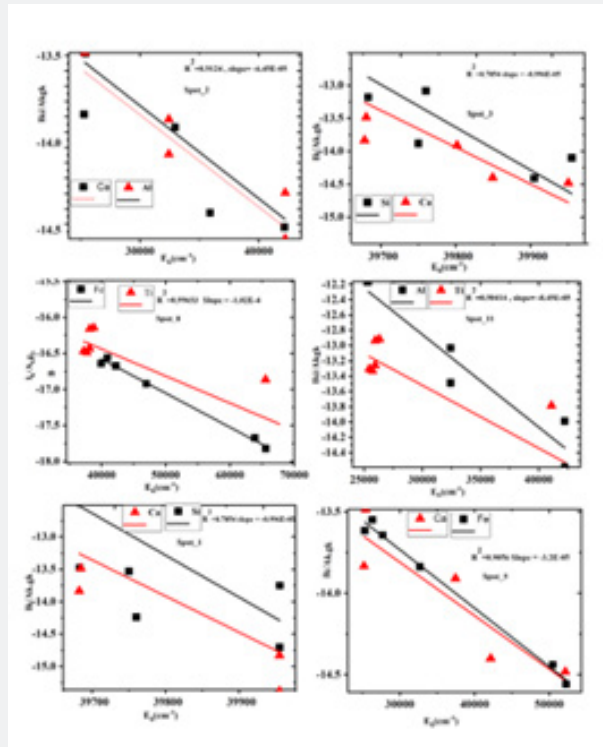


Figure 10: Boltzmann plot of different elements in different spots.

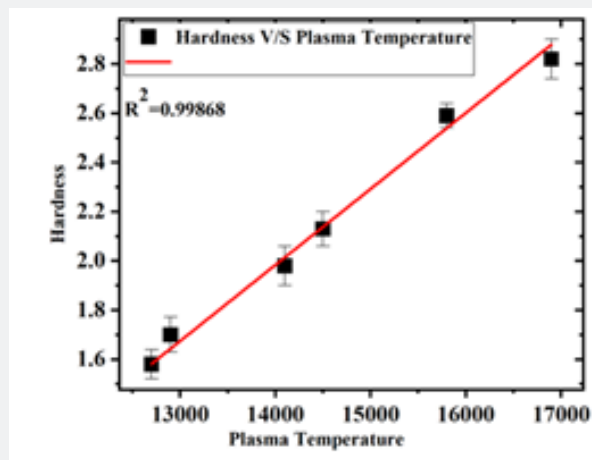


Figure 11: Correlation plot of hardness v/s plasma temperature.

Table 3: Plasma temperature of different location spot.

Sr.No.	Plasma Temperature(K)
Spot_3	15800 ±150
Spot_11	16900 ±280
Spot_1	14500 ±200
Spot_2	13800 ±250
Spot_5	13100±300
Spot_8	12700 ±400

Table 4: Selected spots hardness and their plasma temperatures.

Spot location	Hardness	Plasma Temperature (K)
Spot_3	2.59	14500±200
Spot_11	2.82	16900±280
Spot_1	2.13	14500±200
Spot_2	1.98	13800±250
Spot_5	1.7	13100±300
Spot_8	1.58	12700±400

Table 5: Hardness and electron density of spots.

Spot location	Hardness	Electron density (Ne in cm-3) x1017
Spot_3	2.59	4.68
Spot_11	2.82	4.7
Spot_1	2.13	4.65
Spot_2	1.98	4.6
Spot_5	1.7	4.61
Spot_8	1.58	4.6

Crammers’ et al. [14,32] reported that the breakdown threshold of solids (hardness increase) is lower than that for liquids (loose matrix). Thus, in Granite having a greater hardness value, a minimal part of the leading pulse of the incident laser beam is consumed to attain the breakdown threshold, and the remaining pulse having large energy, is used to heat the plasma resulting in high plasma temperature hence the resultant plasma electron density of plasma increases. In addition to this, due to increase in the temperature, there is the increase of the ionic to atomic line intensity ratio because surface hardness is related to the competition between the ionization and recombination mechanisms in the plasma [26]. Hence, there could be a linear relationship between Plasma electron density, plasma temperature, and hardness. The different hardness spots can be visualized by applying the multivariate technique specially PCA score plot and HCA which can distinguish on the basis of the hardness as discussed in the subsequent section.

Multivariate Technique Analysis

A multivariate technique is used to deliver a qualitative assessment of the LIBS data [33]. Principal component analysis (PCA) is a statistical method and is used in discovering chemical relationships within a complex spectral data set and retain as much information as possible by performing linear regression in multidimensional space. PCA is totally based on finding the principal components describing the major/minor trends in the data set that simplifies the visualization of the distribution of sample, the observation of outliers’ spectra and reduces the variable.

A very standard statistical procedure, Hierarchy clustering analysis (HCA) provides a better alternative for visual representation of high-dimensional data, in this technique an HCA dendrogram incorporates the full dimensionality of the database [34]. HCA groups the analyte vectors according to their inter-vector spatial distances in their full dimensional vector space [35]. The space-wise based HCA, grouped together that data, which has similar profiles chemically/mechanically. HCA is able to organize samples into a tree based on the basis of similarity/dissimilarity of their constituents.

Principal component analysis (PCA)

In this study, the spectroscopic data were analysed statistically via PCA with the help of commercial software (Unscrambler). The twenty-six LIBS spectra of the thirteen different spots (two spectra for each spot were used in the PCA analysis. PCA differentiate and classify the LIBS data in terms of discriminant score plot (Figure 13). The clustering of data point in the score plot (Figure 13) can be explained in terms of hardness. Since, hardness of spot_3, spot_6 and spot_11 is nearly same so these data are clustered positive side with respect to the PC_3 with variance 8%. The spot_5,7,8 & 12 have the lowest hardness value so they are clustered on the negative side with respect to the PC_1 with maximum variance 31%. Remaining all spots such as Spot_1,2,4,9,10 &13 have moderate hardness so these are clustered altogether on the negative side with respect to the PC_1 with a slight amount.

Hierarchy clustering analysis (HCA)

The dendrogram of HCA was employed to envision differences amongst the selected different spots of Granite sample as shown in Figure 14. The twenty-six of the spectral data (intensity v/s wavelength) taking two spectra from each on the basis of the hardness all the spectral data are distributed according to the constituents and their surface morphology. The spot_8,5,7,12 have the same hardness(lowest) and nearly the same morphology so they are clustered in one group. The spot_2,1,4,9,13 have nearly equal hardness(moderate) and hence the same morphology so they are clustered in another group. Spot_3,6&11 have maximum hardness value and nearly equal morphology so they are also formed a separate group (Figure14).

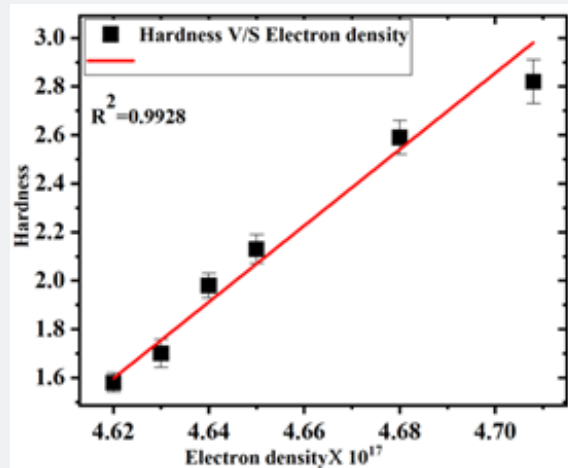


Figure 12: Correlation plot of hardness v/s electron density.

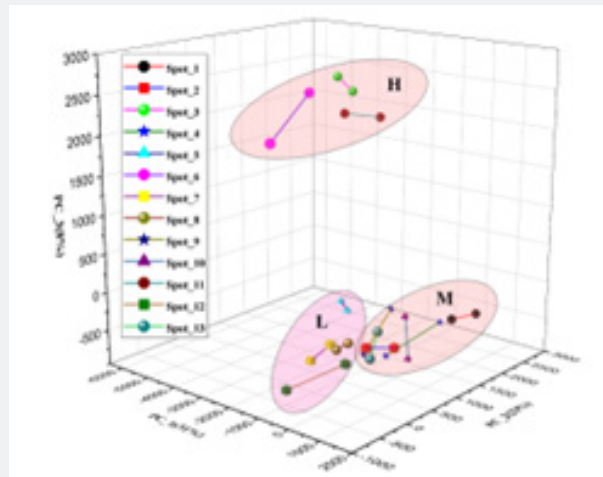


Figure 13: Score plot of each spot of PCA.

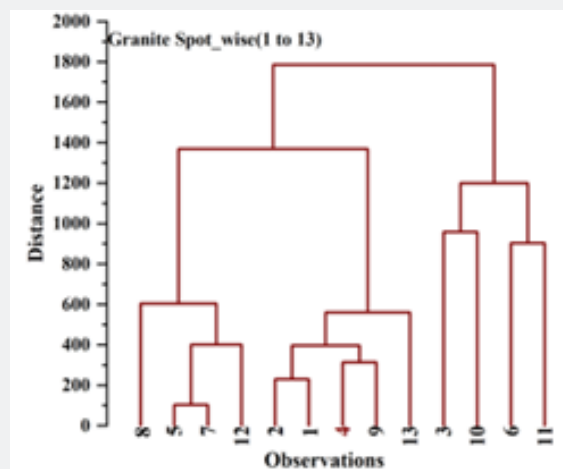


Figure 14: Different spots showing in the dendrogram.

Conclusion

In this paper, Laser-induced breakdown spectroscopy (LIBS) technique is skillfully used to investigate the adverse effect on the environment due to radioactive elements present in multiple hoarded granite and the obtained results successfully supported the geochemical model of radioactive occurrence. The point detection capability of LIBS technique ensured well the presence of radioactive elements such as K_{40} , Th, and U along with common elements Si, Mg, Fe, Ti, Al, Ca, and Li. The color envisioned in each spot was initiated mainly due to the elements Si, Ti, Fe and Ca in various spots of the Granite sample. The hardness of each spot has been obtained by LIBS spectral intensity and compared with the Mohs hardness test. Both results displayed a decent correlation. It was concluded that spots having the maximum hardness value of the granite exhibited minimum occurrence of radioactive elements. Plasma temperature and plasma electron density have crucial relation and has been found that with the increase of the hardness both parameter increases linearly. The chemometric technique such as principal component analysis (PCA) and Hierarchy clustering analysis (HCA) are used to distinguish and explain the distribution of each spot clearly on the basis of hardness of each spot. Both techniques were found in close agreement, and also, both the results were equally supporting the result obtained by the LIBS technique.

References

1. Trumbull RB, Slack JF (2018) Boron isotopes in the continental crust: granites, pegmatites, felsic volcanic rocks, and related ore deposits. *Boron isotopes: The fifth element* 249-272.2.
2. El-Taher A (2012) Elemental analysis of granite by instrumental neutron activation analysis (INAA) and X-ray fluorescence analysis (XRF). *Applied Radiation and Isotopes* 70(1): 350-354.
3. Umar ZA, Ahmed N, Ahmed R, Liaqat U, Baig MA (2018) Elemental composition analysis of granite rocks using LIBS and LA-TOF-MS. *Applied optics* 57: 4985-4991.
4. Adebayo B, Akande J (2011) Textural properties of rock for penetration rate prediction. *Daffodil International University Journal of Science and Technology* 6: 1-8.
5. Bilgin N, Demircin M, Copur H, Balci C, Tuncdemir H, et al. (2006) Dominant rock properties affecting the performance of conical picks and the comparison of some experimental and theoretical results. *International journal of rock mechanics and mining sciences* 43(1): 139-156.
6. Todorovic N, Bikit I, Krmar M, Mrdja D, Hansman J, et al. (2015) Natural radioactivity in raw materials used in building industry in Serbia. *International Journal of Environmental Science and Technology* 12: 705-716.
7. Grdić D, Ristić N, Topličić-Ćurčić G, Krstić D (2018) Potential of usage of self compacting concrete with addition of recycled CRT glass for production of precast concrete elements. *Facta Universitatis, Series: Architecture and Civil Engineering* 16(1): 057-066.
8. Artemieva IM, Thybo H, Jakobsen K, Sorensen NK, Nielsen LS (2017) Heat production in granitic rocks: Global analysis based on a new data compilation GRANITE2017. *Earth-Science Reviews* 172: 1-26.
9. Menager M, Heath M, Ivanovich M, Montjotin C, Barillon C (1993) Migration of uranium from uranium-mineralised fractures into the rock matrix in granite: implications for radionuclide transport around a radioactive waste repository. *Radiochim. Acta* 66: 47-83.
10. Jaupart C, Mareschal J (2005) Constraints on Crustal Heat. *The crust* 3: 65.
11. Van Schmus W (1995) Natural radioactivity of the crust and mantle. In *Global earth physics: A handbook of physical constants*; American Geophysical Union Washington, DC 1: 283-291.
12. Shukla VK, Rai AK, Dwivedi A, Kumar R (2022) A Quick Analysis of Various Elements (Heavy) in Sand Collected from the Topical River (Ganga and Yamuna) Using LIBS Coupled with Multivariate Technique. *National Academy Science Letters* 45(4).
13. Thomas J, Joshi HC (2023) Review On Laser Induced Breakdown spectroscopy: Methodology and Technical Developments. *arXiv preprint arXiv:2302.13272*.
14. Cremers DA, Radziemski LJ (2013) *Handbook of laser-induced breakdown spectroscopy*; John Wiley & Sons.
15. Ismail MA, Imam H, Elhassan A, Youniss WT, Harith MA (2004) LIBS limit of detection and plasma parameters of some elements in two different metallic matrices. *Journal of analytical atomic spectrometry* 19(4): 489-494.
16. Krasniker R, Bulatov V, Schechter I (2001) Study of matrix effects in laser plasma spectroscopy by shock wave propagation. *Spectrochimica Acta Part B: Atomic Spectroscopy* 56(6): 609-618.
17. Quinn GD (2006) Fracture toughness of ceramics by the Vickers indentation crack length method: a critical review. *Mechanical properties and performance of engineering ceramics II: Ceramic engineering and science proceedings* 27: 45-62.
18. Shahdad SA, McCabe JF, Bull S, Rusby S, Wassell RW (2007) Hardness measured with traditional Vickers and Martens hardness methods. *Dental Materials* 23(9): 1079-1085.
19. Al-Najjar O, Wudil Y, Ahmad U, Baghabra Al-Amoudi OS, Al-Osta MA (2022) Applications of laser induced breakdown spectroscopy in geotechnical engineering: a critical review of recent developments, perspectives and challenges. *Applied Spectroscopy Reviews*: 1-37.
20. Abdel-Salam Z, Galmed A, Tognoni E, Harith M (2007) Estimation of calcified tissues hardness via calcium and magnesium ionic to atomic line intensity ratio in laser induced breakdown spectra. *Spectrochimica Acta Part B: Atomic Spectroscopy* 62(12): 1343-1347.
21. ElFaham MM, Okil M, Mostafa AM (2018) Limit of detection and hardness evaluation of some steel alloys utilizing optical emission spectroscopic techniques. *Optics & Laser Technology* 108: 634-641.
22. Tsuyuki K, Miura S, Idris N, Kurniawan KH, Lie TJ (2006) Measurement of concrete strength using the emission intensity ratio between Ca (II) 396.8 nm and Ca (I) 422.6 nm in a Nd: YAG laser-induced plasma. *Applied spectroscopy* 60: 61-64.
23. Granato D, Santos JS, Escher GB, Ferreira BL, Maggio RM (2018) Use of principal component analysis (PCA) and hierarchical cluster analysis (HCA) for multivariate association between bioactive compounds and functional properties in foods: A critical perspective. *Trends in Food Science & Technology* 72: 83-90.
24. Ralchenko Y (2005) NIST atomic spectra database, *Memorie della Societa Astronomica Italiana Supplementi* 8: 96.
25. White RE (2005) *Principles and practice of soil science: the soil as a natural resource*; John Wiley & Sons.
26. Aberkane SM, Bendib A, Yahiaoui K, Boudjemai S, Abdelli-Messaci S (2014) Correlation between Fe-V-C alloys surface hardness and plasma temperature via LIBS technique. *Applied surface science* 301: 225-229.

27. Ghorbani S, Hoseinie SH, Ghasemi E, Sherizadeh T, Wanhainen CA (2022) new rock hardness classification system based on portable dynamic testing. *Bulletin of Engineering Geology and the Environment* 81: 179.
28. Clauser C (2009) Heat transport processes in the Earth's crust. *Surveys in Geophysics* 30: 163-191.
29. Sattar H, Ran H, Ding W, Imran M, Amir M (2020) An approach of stand-off measuring hardness of tungsten heavy alloys using LIBS. *Applied Physics B* 126: 1-11.
30. Shukla PK, Mamun A (2015) *Introduction to dusty plasma physics*; CRC press:.
31. Bakhtiyari AN, Wu Y, Qin D, Zheng H (2023) Modeling temporal and spatial evolutions of laser-induced plasma characteristics by using machine learning algorithms. *Optik* 272: 170297.
32. Rai V, Thakur S (2007) Physics of plasma in laser-induced breakdown spectroscopy. *Laser-induced breakdown spectroscopy* 83-111.
33. Adarsh U, Kartha V, Santhosh C, Unnikrishnan V (2022) Spectroscopy: A promising tool for plastic waste management. *TrAC Trends in Analytical Chemistry* 149: 116534.
34. Zhang C, Bailey DP, Suslick KS (2006) Colorimetric sensor arrays for the analysis of beers: A feasibility study. *Journal of agricultural and food chemistry* 54: 4925-4931.
35. Altman N, Krzywinski M (2017) Points of significance: clustering. *Nature methods* 14(6): 545-547.



This work is licensed under Creative Commons Attribution 4.0 License
DOI: [10.19080/IMST.2023.04.5556231](https://doi.org/10.19080/IMST.2023.04.5556231)

**Your next submission with Juniper Publishers
will reach you the below assets**

- Quality Editorial service
- Swift Peer Review
- Reprints availability
- E-prints Service
- Manuscript Podcast for convenient understanding
- Global attainment for your research
- Manuscript accessibility in different formats
(Pdf, E-pub, Full Text, Audio)
- Unceasing customer service

Track the below URL for one-step submission

<https://juniperpublishers.com/online-submission.php>